The role of collagen in extralobar pulmonary artery stiffening in response to hypoxia-induced pulmonary hypertension

Chen Yen Ooi, Zhijie Wang, Diana M. Tabima, Jens C. Eickhoff and Naomi C. Chesler

You might find this additional info useful...

This article cites 47 articles, 25 of which can be accessed free at:
http://ajpheart.physiology.org/content/299/6/H1823.full.html#ref-list-1

Updated information and services including high resolution figures, can be found at:
http://ajpheart.physiology.org/content/299/6/H1823.full.html

Additional material and information about *AJP - Heart and Circulatory Physiology* can be found at:
http://www.the-aps.org/publications/ajpheart

This infomation is current as of January 17, 2011.

The role of collagen in extralobar pulmonary artery stiffening in response to hypoxia-induced pulmonary hypertension

Chen Yen Ooi,[1] Zhijie Wang,[1] Diana M. Tabima,[1] Jens C. Eickhoff,[2] and Naomi C. Chesler[1]

Departments of [1]Biomedical Engineering and [2]Biostatistics and Medical Informatics, University of Wisconsin-Madison, Madison, Wisconsin

Ooi CY, Wang Z, Tabima DM, Eickhoff JC, Chesler NC. The role of collagen in extralobar pulmonary artery stiffening in response to hypoxia-induced pulmonary hypertension. *Am J Physiol Heart Circ Physiol* 299: H1823–H1831, 2010. First published September 17, 2010; doi:10.1152/ajpheart.00493.2009.—Hypoxic pulmonary hypertension (HPH) causes extralobar pulmonary artery (PA) stiffening, which potentially impairs right ventricular systolic function. Changes in the extracellular matrix proteins collagen and elastin have been suggested to contribute to this arterial stiffening. We hypothesized that vascular collagen accumulation is a major cause of extralobar PA stiffening in HPH and tested our hypothesis with transgenic mice that synthesize collagen type I resistant to collagenase degradation ($Col1a1^{R/R}$). These mice and littermate controls that have normal collagen degradation ($Col1a1^{+/+}$) were exposed to hypoxia for 10 days; some were allowed to recover for 32 days. In vivo PA pressure and isolated PA mechanical properties and collagen and elastin content were measured for all groups. Vasoactive studies were also performed with U-46619, Y-27632, or calcium- and magnesium-free medium. Pulmonary hypertension occurred in both mouse strains due to chronic hypoxia and resolved with recovery. HPH caused significant PA mechanical changes in both mouse strains: circumferential stretch decreased, and mid-to-high-strain circumferential elastic modulus increased ($P < 0.05$ for both). Impaired collagen type I degradation prevented a return to baseline mechanical properties with recovery and, in fact, led to an increase in the low and mid-to-high-strain moduli compared with hypoxia ($P < 0.05$ for both). Significant changes in collagen content were found, which tended to follow changes in mid-to-high-strain elastic modulus. No significant changes in elastin content or vasoactivity were observed. Our results demonstrate that collagen content is important to extralobar PA stiffening caused by chronic hypoxia.

biomechanics; mechanobiology; elastin; hydroxyproline; recovery

HYPOXIC PULMONARY HYPERTENSION (HPH) is caused by living at high altitudes and is a complication of many lung diseases, including chronic obstructive pulmonary disease (1, 13, 16), cystic fibrosis (10), and obstructive sleep apnea (13), which contributes significantly to morbidity and mortality. Pulmonary vascular remodeling due to chronic HPH increases conduit pulmonary artery (PA) stiffness (4, 20, 21, 23, 34, 42). Conduit PA stiffening likely increases wave reflections to impair right ventricular systolic function, much like aortic stiffening impairs left ventricular systolic function (18, 29, 33). Our laboratory has previously shown that HPH increases wave reflections in the mouse pulmonary circulation (44). Recent evidence showing that conduit PA stiffness is a strong predictor of mortality in PA hypertension (12, 30) further supports the

importance of PA stiffness to pulmonary and right ventricular function.

The dominant morphological changes in conduit PAs in response to HPH are accumulation of collagen and elastin (20, 21) and wall thickening (4, 20, 21, 23). Stiffening of the extralobar PAs has been shown to be linked with accumulation of collagen and elastin (4, 20, 21, 23, 42). Previous attempts to understand the individual roles of collagen and elastin in arterial mechanical function have focused on correlative relationships during HPH progression (20, 21) or ex vivo degradation of one component before mechanical testing (23). A disadvantage of the first approach is that, if elastin also increases during HPH progression, the impact of either protein alone cannot be discerned; a disadvantage of the second approach is that degradation of one component may alter potentially important interactions between the two (9).

We sought a novel way to test our hypothesis that vascular collagen accumulation is a major cause of extralobar PA stiffening in HPH. To do so, we used a strain of mouse genetically engineered to have collagenase-resistant type I collagen (Col1a1). We predicted that this defect would allow us to create a condition in which changes in vascular collagen content were decoupled from other changes in the pulmonary vasculature caused by hypoxia. Type I collagen is a fibrillar collagen subtype that plays a dominant role in the composition and strength of arteries (3, 14). The amount of the type I collagen in an artery is regulated by the activities of matrix metalloproteinases (MMPs) and tissue inhibitors of MMPs (35). COL1A1 is the gene that encodes for the α1 chains of the triple helix type I collagen molecules (46). The homozygous collagenase-resistant Col1a1 mouse ($Col1a1^{R/R}$) synthesizes collagen type I that is resistant to collagenase cleavage between Gly775 and Ile776 sites of the α1 chains, which is the site of action of human MMPs (28). This collagen degradation-resistant property of the $Col1a1^{R/R}$ mice has been shown to cause dermal fibrosis (28), impaired postpartum involution of the uterus (28), and impaired wound healing (2). Homozygous Col1a1 mice that do not show the mutant characteristic are classified as $Col1a1^{+/+}$; in these animals collagen type I is degraded normally.

In this study, $Col1a1^{+/+}$ and $Col1a1^{R/R}$ mice were made chronically hypoxic to promote vascular collagen accumulation; some were allowed to recover to decouple collagen content from other pulmonary vascular changes. Mechanical and biological properties of extralobar PAs were examined. We predicted that the PA collagen content would increase with exposure to hypoxia in both $Col1a1^{+/+}$ and $Col1a1^{R/R}$ mice, resulting in PA stiffening. With recovery, we anticipated that the collagen content would decrease to near-normal levels in $Col1a1^{+/+}$ mice, returning arterial stiffness to normal levels. In

Address for reprint requests and other correspondence: N. C. Chesler, Associate Professor of Biomedical Engineering, Univ. of Wisconsin at Madison, 2146 Engineering Centers Bldg., 1550 Engineering Dr., Madison, WI 53706-1609 (e-mail: chesler@engr.wisc.edu).

contrast, the vascular collagen content in Col1a1$^{R/R}$ mice was expected to remain high after recovery, resulting in a persistent elevation in arterial stiffness. This experimental strategy was designed to allow us to investigate the role of collagen in extralobar PA stiffening in HPH.

MATERIALS AND METHODS

Animal handling. Breeding pairs of Col1a1^{tmJae} mice (28) on the B6/129 background were obtained from Jackson Laboratory (Bar Harbor, ME). Genotyping by polymerase chain reaction was performed on DNA extracted from tail biopsies (Wizard SV Genomic DNA Purification System, Promega, Madison, WI) using primers indicated in the strain information provided by the Jackson Laboratory, as previously described (49).

Col1a1$^{+/+}$ and Col1a1$^{R/R}$ mice were randomized into three groups: 42 days of normoxia (normoxia), 32 days of normoxia followed by 10 days of hypoxia (hypoxia), and 10 days of hypoxia followed by 32 days of recovery (recovery). The randomization was stratified by sex to ensure approximately equal numbers of male and female mice for each group. All mice were 16–18 wk old at the time of euthanization. Hypoxia was created in an environmentally controlled chamber in which nitrogen was mixed with laboratory air until an oxygen concentration of 10% was reached; oxygen levels were measured with a sensor in the chamber (Servoflo, Lexington, MA) and used to control a relay valve on the nitrogen gas inflow line via a custom-built closed-loop control system. The flow rate of the (constant flow) air mixture was adjusted to maintain the carbon dioxide level at <600 ppm. Mice in the normoxia and recovery conditions were placed in identical environmental chambers with the same overall airflow, but without forced nitrogen (21% O_2). Temperature, oxygen and carbon dioxide concentrations, and humidity were checked daily. Twelve-hour on/off light conditions and normal diet and water were provided. The chambers were opened for no more than 30 min once per 2 days for regular animal care and maintenance. All procedures were approved by the University of Wisconsin-Madison Institutional Animal Care and Use Committee.

In vivo pressure measurement. In vivo pressure measurements were conducted to confirm development of HPH in response to chronic hypoxia and resolution of HPH after an extended period of normoxia. The mice were anesthetized with urethane (1 mg/g intraperitoneal), intubated, and placed on a ventilator (Harvard Apparatus, Holliston, MA). The apex of the right ventricle was localized after removing the chest wall, and a 1.4 F pressure-tip catheter (Millar Instruments, Houston, TX) was introduced using a 20-gauge needle. After instrumentation was established and right ventricular pressure readings were stable, the catheter was advanced to main PA. PA pressure was recorded and analyzed with commercially available software (Notocord, Croissy Sur Seine, France) with the animal breathing room air.

Isolated vessel mechanical testing. Mice were euthanized with an overdose of 50 mg/ml pentobarbital by intraperitoneal injection. Then a midline sternotomy was performed, and the heart and lungs were removed. Extralobar conduit PAs were harvested from the pulmonary trunk to the first branches under microscopy. Left PAs were used for mechanical testing and saved for histology after testing.

The mechanical testing system was set up as shown in Fig. 1. PAs were mounted on 410-μm-diameter glass cannulas in a vessel chamber [Living System Instrumentation (LSI), Burlington, VT]. Care was taken to avoid vessel collapse during harvest and mounting. Desired pressures were applied by perfusion of physiological saline solution (PSS) using a servo-control pump (LSI). Pressure transducers were placed in-line next to the cannulas to record pressures on both sides of the vessel. The average pressure, P, was used for all material and mechanical property calculations. A charge-coupled device camera (IonOptix, Milton, MA) connected to an inverted microscope (Olympus, Center Valley, PA) was used to take images of the vessel at ×4 magnification. These images were sent to a video dimension analyzer
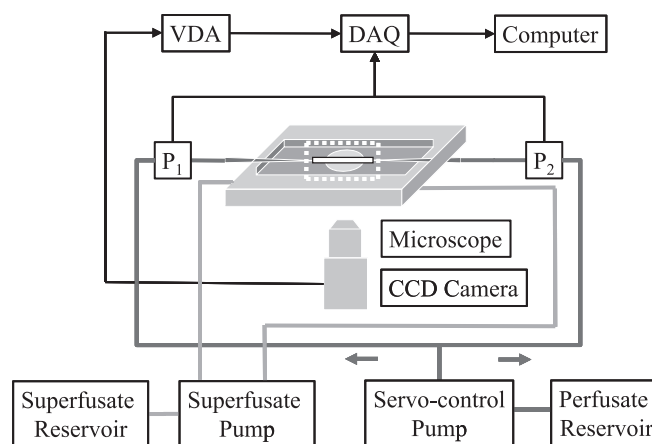

Fig. 1. Isolated vessel mechanical testing system. VDA, video dimension analyzer; DAQ, data-acquisition system; CCD, charge-coupled device; P_1 and P_2, pressure transducers from which average intravascular pressure $P = (P_1 + P_2)/2$ was calculated.

(LSI) for automatic detection of outer diameter (OD) along a single line at the approximate middle, lengthwise, of the vessel. A superfusate pump (Ismatec, Glattbrugg, Switzerland) was used to provide pH-adjusted PSS (pH = 7.4) at 37°C in the vessel bath.

Immediately after mounting, the PAs were pressurized to 5 mmHg. The unstretched lengths were measured from suture to suture, and then the vessels were stretched 140% to prevent buckling at higher pressures. The average unstretched length of the harvested PAs was 1.98 ± 0.04 mm, with no differences between strain or exposure condition. Cannula ends were held fixed so that all testing was performed with a constant vessel length. Next, PAs were allowed to equilibrate at 15 mmHg for 30 min. Wall thickness (*h*) was measured at higher magnification (×10) at three different transmural pressures: 5, 30, and 60 mmHg. After another 30-min equilibrium, sinusoidal pressurization cycles from 15 to 30 mmHg and 45 to 60 mmHg (10 cycles for each pressure range) were applied at 1 Hz for preconditioning. Then pressure steps of 15, 20, 30, 40, 50, 60, and 15 mmHg were applied for 45 s each after a resting pressurization at 5 mmHg for 450 s. The vessels were allowed to rest for 10 times the loading period between each step to reduce the effects of viscoelasticity (22). Vessel plastic deformation was checked at the final 15-mmHg step. Insignificant differences in OD (<1%) compared with the first 15-mmHg step were observed, indicating absence of plastic deformation. Pressure and OD were sampled at 1 Hz through LabView (National Instruments, Austin, TX) and sent to a data-acquisition system (National Instruments). OD measured at 40 s into each step was used for the mechanical property calculations.

Vasoactive experiments were also performed in which vessels were treated with a potent vasoconstrictor U-46619 (4.5 × 10^{-7} M; Cayman Chemical, Ann Arbor, MI), vasodilator Y-27632 (1 × 10^{-5} M; Sigma-Aldrich, St. Louis, MO), or a calcium- and magnesium-free medium (MP Biomedicals, Solon, OH) at a fixed pressure of 15 mmHg.

Mechanical properties calculation. The arteries were assumed to be at a fixed length, homogeneous, and incompressible (20, 21, 36). The overall stiffness is represented by circumferential stretch (λ) at each pressure:

$$\lambda = \frac{\pi \times OD}{\pi \times OD_5} = \frac{OD}{OD_5} \qquad (1)$$

where OD_5 is the OD at 5 mmHg to approximate the no-load state.

Assuming conservation of mass and no axial extension (8), the *h* as a function of pressure was calculated as:

$$h = \frac{1}{2}\Big[OD - \sqrt{OD^2 - OD_{60}^2 + (OD_{60} - 2h_{60})^2}\Big] \qquad (2)$$

where OD_{60} and h_{60} are the OD and h measured at 60 mmHg, respectively.

Midwall stress (σ) and strain (ε) were calculated using the thin-walled assumption and Green's formulation for finite deformation, respectively:

$$\sigma = P\frac{D_m}{2h} \qquad (3)$$

$$\varepsilon = \frac{1}{2}\left(\frac{D_m^2}{D_{m5}^2} - 1\right) \qquad (4)$$

where D_m is the midwall diameter, and D_{m5} is the midwall diameter at 5 mmHg. The advantage of choosing the midwall stress and strain is that the no-load state can be used as the reference state instead of the zero-stress state (48). From the obtained stress-strain curves, elastic modulus at low strain (E_1) was calculated as the slope of the curve for $0 \le \varepsilon \le 1.0$, and the modulus at mid-to-high strain (E_2) was calculated as the slope for $1.0 \le \varepsilon \le 1.6$. We did not compute a high-strain modulus as done previously (20), because moduli are most appropriately compared over the same strain range, and the maximum strains found here for each group were quite different. The $1.0 \le \varepsilon \le 1.6$ range allowed us to calculate an elastic modulus for all six groups. At higher strain, we could only calculate moduli for the normoxic groups.

Vasoactivity analysis. In response to treatment with the vasoconstrictor U-46619, the vasodilator Y-27632, or the calcium- and magnesium-free medium, the percent changes of the diameter were calculated as:

$$\%\text{changes} = \frac{OD - OD_N}{OD_N} \times 100\% \qquad (5)$$

where OD is in response to the drug, and OD_N is the OD at a normal tone state (PSS alone) at the same pressure.

Biochemical assays. To correlate the mechanical behavior with collagen and elastin content, biochemical assays were performed on left and right PAs from additional groups of mice. Tissue homogenates were assayed for hydroxyproline (OHP) content, which is one of the most abundant amino acids in collagen and is often used as a marker for collagen content (39), using standard techniques (5, 47). The Fastin elastin assay (Biocolor, Carrickfergus, UK) was performed according to the manufacturer's instructions. The total tissue OHP and elastin content are presented as micrograms per vessel.

Histology. After mechanical testing, left PAs were fixed in 10% formalin at 15 mmHg and preserved in 70% ethanol. The vessels were then embedded in agar gel, sectioned, and stained with picrosirius red.

Statistics. All results are presented as means ± SE. The association between PA stretch and exposure condition was analyzed using a linear mixed-effect model with repeated measures (generalized least squares). For each mouse strain, a two-way comparison of factors was performed (exposure condition and pressure), which led to the construction of contrast matrices that were used to investigate changes in stretch as functions of these factors. No violations of the normality assumption were found. The Benjamini-Hochberg method was used to adjust for multiple comparisons between exposure conditions. A compound symmetry correlation structure was assumed between repeated measurements.

In vivo pressures, h, E_1, E_2, vasoactivity, and biochemical results were analyzed by two-way ANOVA and Tukey's multiple comparisons. Goodness of fit was evaluated by computing Akaike's information criterion measures. Model assumptions were validated using standard model validation techniques.

The nonparametric Spearman rank correlation test with a permutation analysis (permutation size M = 10,000) was used to compute the Spearman's correlation coefficient (r_s) and P values for correlations between the averages of E_1 or E_2, and averages of collagen or elastin content for both strains combined using SAS version 9.2. To assess linearity, a simple linear correlation coefficient (R^2) was determined for the averages of E_1 or E_2, and averages of collagen or elastin content for both strains combined using Microsoft Excel.

All other analyses were performed using R (http://www.r-project.org/) version 2.5.1. $P < 0.05$ was considered significant.

RESULTS

In vivo pressure. In response to hypoxia, PA systolic pressure increased for both Col1a1$^{+/+}$ and Col1a1$^{R/R}$ mice ($P < 0.01$, Table 1). With recovery, PA systolic pressures of both strains decreased ($P < 0.05$). In the normoxic condition, the Col1a1$^{R/R}$ mice had lower PA pressures than Col1a1$^{+/+}$ mice ($P < 0.05$) and had a larger relative increase in mean PA pressure with exposure to hypoxia (25% increase for Col1a1$^{+/+}$ vs. 56% increase for Col1a1$^{R/R}$). With recovery, mean PA pressure decreased by a similar amount in both strains (~24%), which brought the Col1a1$^{+/+}$ mice PA pressure back to normal levels, but left the Col1a1$^{R/R}$ mice with a slight elevation in mean PA pressure. The heart rate under anesthesia with urethane was not affected by strain or exposure condition (Table 1).

Diameter and wall thickness. The OD of Col1a1$^{+/+}$ PAs at 5 mmHg were 592 ± 19, 607 ± 11, and 575 ± 8 μm in the normoxic, hypoxic, and recovery groups, respectively. In Col1a1$^{R/R}$, these values were 561 ± 19, 578 ± 15, and 604 ± 9 μm, respectively. No differences were significant. To assess physiologically relevant wall thickening, we compared h measured optically at 30 mmHg (Fig. 2). The increases in h with hypoxia in both strains were significant ($P < 0.001$), as were the decreases with recovery ($P < 0.01$ vs. hypoxia). No significant differences were found between the two strains for

Table 1. *HR and PA pressures obtained in vivo*

Mouse Strain	Exposure	HR, beats/min	PA Pressure, mmHg		
			Systolic	Diastolic	Mean
Col1a1$^{+/+}$	Normoxia	577 ± 16	28.7 ± 2.0	16.7 ± 1.8	22.1 ± 2.0
	Hypoxia	577 ± 26	36.9 ± 1.3*	19.6 ± 2.3	27.6 ± 1.7
	Recovery	570 ± 13	29.2 ± 0.6†	15.0 ± 1.1	21.1 ± 0.5
Col1a1$^{R/R}$	Normoxia	528 ± 45	22.1 ± 0.8‡	10.4 ± 0.4‡	15.6 ± 0.6‡
	Hypoxia	586 ± 12	31.9 ± 1.6*	18.6 ± 1.5*	24.4 ± 1.4*
	Recovery	551 ± 22	24.8 ± 1.0†	13.2 ± 2.1	18.4 ± 1.6

Values are means ± SE; N = 5–7 per group. HR, heart rate; PA, pulmonary artery. $P < 0.05$ for *hypoxia or recovery vs. normoxia, †recovery vs. hypoxia, and ‡Col1a1$^{R/R}$ vs. Col1a1$^{+/+}$.
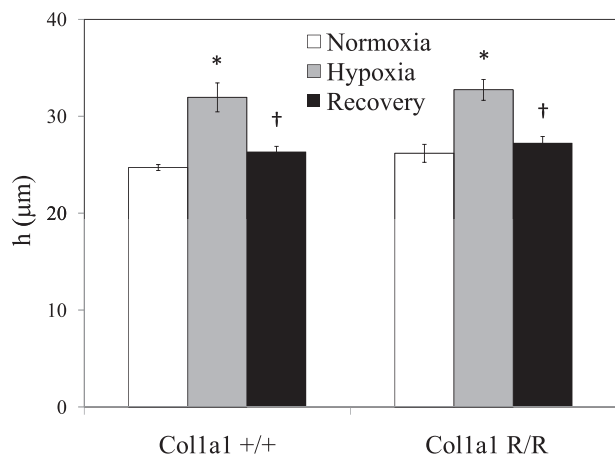
Fig. 2. Pulmonary artery (PA) wall thickness (h) measured at 30 mmHg. Col1a1, collagenase-resistant type I collagen. Values are means ± SE; N = 7–12 per group. $P < 0.05$ for *hypoxia or recovery vs. normoxia, and †recovery vs. hypoxia.

any exposure condition. Histology images also showed medial and adventitial thickening with hypoxia and thinning with recovery in both mouse strains (Fig. 3).

Stretch and elastic moduli. PA circumferential stretch was analyzed to compute the vessel overall stiffness, where lower stretch at a given pressure indicates a stiffer vessel. As shown in Fig. 4, PA circumferential stretch decreased with hypoxia in both Col1a1$^{+/+}$ and Col1a1$^{R/R}$ mice ($P < 0.001$ for pressures ≥ 20 mmHg vs. normoxia). With recovery, the stretch of Col1a1$^{+/+}$ PAs significantly increased compared with the hypoxic condi-

tion, but was still lower than that of the normoxia group ($P < 0.01$ for pressures ≥ 20 mmHg vs. hypoxia and normoxia). In contrast, Col1a1$^{R/R}$ PA stretch in recovery remained at a similar level to that of the hypoxia group ($P < 0.001$ for pressures ≥ 20 mmHg vs. normoxia).

The circumferential stress-strain relationships were obtained for both strains of mice (Col1a1$^{+/+}$ and Col1a1$^{R/R}$) for the three different exposure conditions (normoxia, hypoxia, and recovery) (Fig. 5). In the Col1a1$^{+/+}$ mice, hypoxia shifted the stress-strain curve leftward, indicating stiffening of the artery, and recovery shifted the curve rightward, toward normoxia. The same leftward shift occurred in the Col1a1$^{R/R}$ mice with hypoxia; however, during recovery, the curve was further shifted leftward, indicating additional stiffening of the artery.

We compared tangent elastic moduli of these stress-strain curves for fixed strain ranges in which there was significant overlap between groups. In particular, we calculated a low-strain tangent circumferential elastic modulus for $0 \leq \varepsilon \leq 1.0$ (E_1) and a mid-to-high-strain modulus for $1.0 \leq \varepsilon \leq 1.6$ (E_2). As shown in Fig. 6, E_1 did not vary significantly except with recovery in Col1a1$^{R/R}$ mice. In contrast, E_2 increased with hypoxia and decreased with recovery in the Col1a1$^{+/+}$ mice and increased with hypoxia and increased further with recovery in the Col1a1$^{R/R}$ mice (all $P < 0.001$).

Between mouse strains, E_1 and E_2 were similar in the normoxic condition. However, E_2 increased less with hypoxia for the Col1a1$^{R/R}$ PAs than the Col1a1$^{+/+}$ PAs. With recovery, E_2 was much greater in the Col1a1$^{R/R}$ mice than in the Col1a1$^{+/+}$ mice ($P < 0.001$), and E_1 was increased as well ($P < 0.05$).
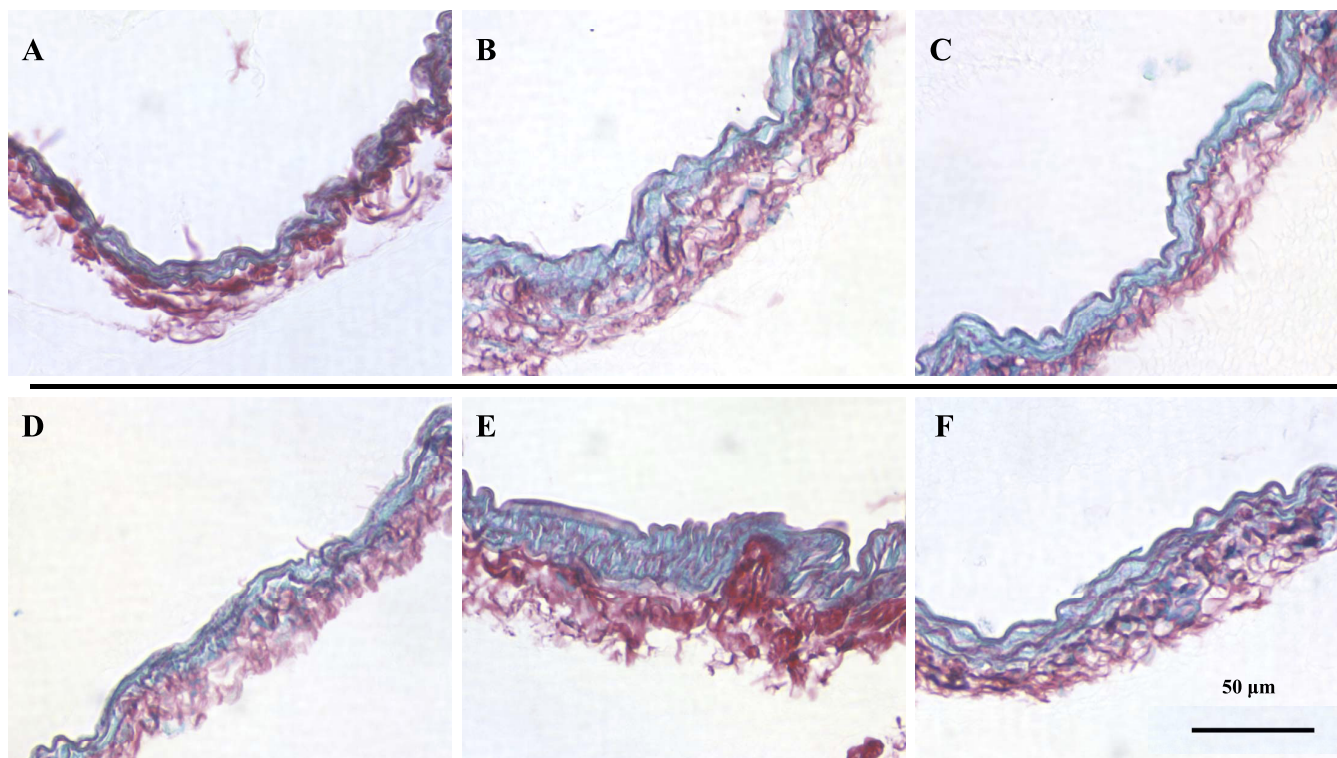
Fig. 3. Representative histology images of the PAs of Col1a1$^{+/+}$ mice exposed to normoxia (*A*), hypoxia (*B*), and recovery (*C*), and Col1a1$^{R/R}$ mice exposed to normoxia (*D*), hypoxia (*E*), and recovery groups (*F*). Collagen is stained red. For all images, the scale bar is the same (see *F*); the lumen faces the *top* of the image, and the adventitia faces the *bottom*.
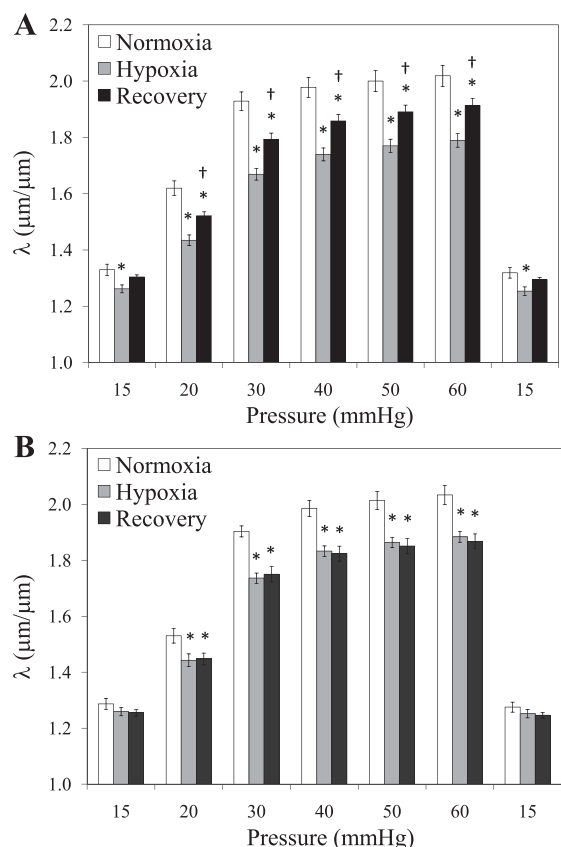
Fig. 4. Stretch (λ) of PAs of Col1a1$^{+/+}$ (*A*) and Col1a1$^{R/R}$ (*B*) mice exposed to normoxia, hypoxia, and recovery. Values are means $\pm$ SE; $N = 7$–12 per group. $P < 0.05$ for *hypoxia or recovery vs. normoxia, and †recovery vs. hypoxia.

essentially no relationships between E_1 and elastin content ($R^2 = 0.19$, $r_s = 0.03$, $P = 0.83$; Fig. 8*A*), E_1 and collagen content ($R^2 = 0.05$, $r_s = 0.06$, $P = 0.79$), or E_2 and elastin content ($R^2 = 0.23$, $r_s = -0.11$, $P = 0.73$). E_2 and collagen content showed a linear relationship ($R^2 = 0.87$), but the correlation was not significant ($r_s = 0.46$, $P = 0.39$) due to the large standard errors for each group mean (Fig. 8*B*), which were taken into account with the permutation analysis.

DISCUSSION

The present study demonstrates that HPH significantly increases collagen content and mid-to-high-strain elastic modulus in extralobar PAs and that impaired degradation of collagen type I leads to even greater increases in collagen content and elastic modulus during recovery.

Hypoxia-induced pulmonary hypertension. Measurements of in vivo PA pressure indicate the successful development of pulmonary hypertension with hypoxia in both Col1a1$^{+/+}$ and Col1a1$^{R/R}$ mice, as shown by numerous other studies with other strains of mice (7, 25, 31). Interestingly, in the normoxic condition, the Col1a1$^{R/R}$ mice had lower mean PA pressures than Col1a1$^{+/+}$ mice and had a larger relative increase in mean PA pressure with exposure to hypoxia. In response to hypoxia, distal arteriolar muscularization and narrowing are largely responsible for increases in mean PA pressure and pulmonary vascular resistance (44). Collagen degradation is known to play an active role in this process; in particular, mRNA levels of
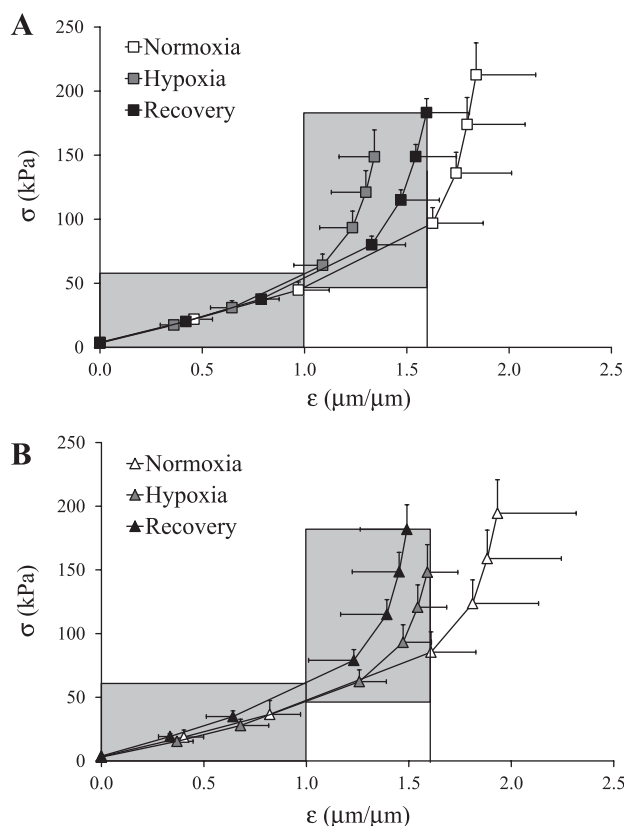
Vasoactivity. Significant constriction was observed in response to treatment with U-46619 for all groups ($P < 0.01$ vs. normal tone state). On average, the percent change in diameter was -35% with no significant differences between groups (Col1a1$^{+/+}$ normoxia -29 ± 4, hypoxia -36 ± 3, recovery $-37 \pm 6\%$; Col1a1$^{R/R}$ normoxia -36 ± 6, hypoxia -34 ± 5, recovery $-38 \pm 3\%$; $n = 6$–8 per group). No significant changes in diameter were found for any groups in response to treatment with Y-27632 or calcium- and magnesium-free medium ($P \approx 1$ vs. normal tone state; $n = 4$–8 per group).

OHP/collagen and elastin content. OHP content of both Col1a1$^{+/+}$ and Col1a1$^{R/R}$ PAs increased with hypoxia, but the changes reached significance only in Col1a1$^{+/+}$ mice ($P < 0.05$; Fig. 7). After recovery, the OHP content of the Col1a1$^{+/+}$ PAs tended to decrease, whereas OHP in the Col1a1$^{R/R}$ PAs increased further and became higher than that in the normoxic group ($P < 0.05$). The elastin content of Col1a1$^{+/+}$ PAs for normoxia, hypoxia, and recovery were 9.86 ± 2.11, 8.77 ± 1.52, and 10.68 ± 1.77 µg/vessel, respectively, and that of Col1a1$^{R/R}$ PAs for normoxia, hypoxia, and recovery were 10.52 ± 2.32, 8.14 ± 0.64, and 9.91 ± 0.79 µg/vessel, respectively ($n = 4$–9 per group). The differences in elastin content between exposures and between the two mouse strains were not significant, and no trends were evident.

Mechanobiological correlations. The PA structure-function relationships were further assessed by correlating E_1 and E_2 with the elastin and collagen (OHP) content. There were

Fig. 5. Midwall stress (σ) vs. strain (ε) curves of PAs of Col1a1$^{+/+}$ (*A*) and Col1a1$^{R/R}$ (*B*) mice exposed to normoxia, hypoxia, and recovery. The shaded areas are the two strain ranges in which we calculated elastic moduli E_1 and E_2. Values are means $\pm$ SE; $N = 7$–12 per group.
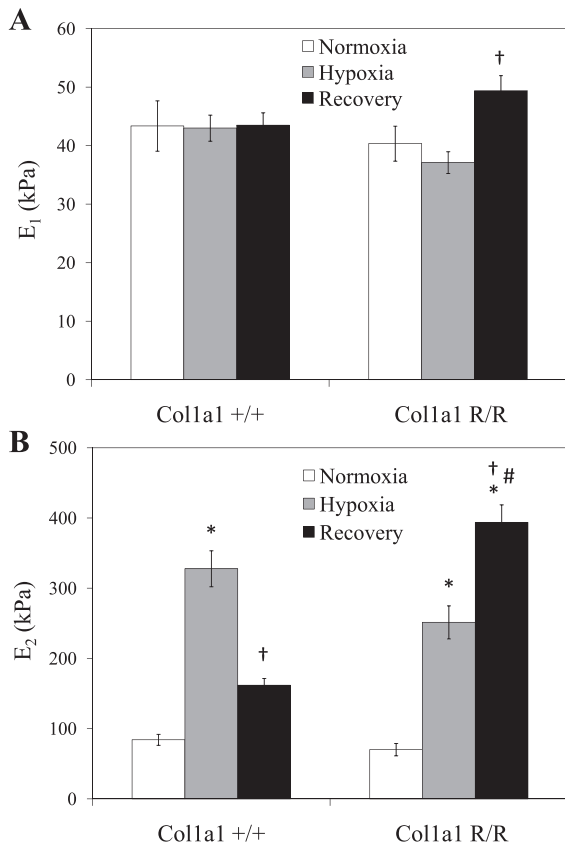
Fig. 6. Tangent circumferential elastic moduli E_1 (A) and E_2 (B) of PAs of Col1a1$^{+/+}$ and Col1a1$^{R/R}$ mice exposed to normoxia, hypoxia, and recovery. Values are means ± SE; $N = 7$–12 per group. $P < 0.05$ for *hypoxia or recovery vs. normoxia, †recovery vs. hypoxia, and #Col1a1$^{R/R}$ vs. Col1a1$^{+/+}$.

Fig. 8. Mechanobiological correlations between E_1 and elastin content (A) and E_2 and collagen (OHP) content (B). Values are means ± SE.

MMP-8, which has substrate affinity for fibrillar collagens type I and III, increases rapidly and significantly in response to chronic hypoxia (6). The inability of this enzyme to degrade collagen type I in the Col1a1$^{R/R}$ mice may play a role in the relatively large increase in PA pressure in this strain.

With recovery, the PA pressures of the Col1a1$^{+/+}$ mice returned to normal levels, as previously shown to occur in rats (26, 27, 38). In the Col1a1$^{R/R}$ mice, the mean PA pressures after recovery tended to be higher than normal levels, which
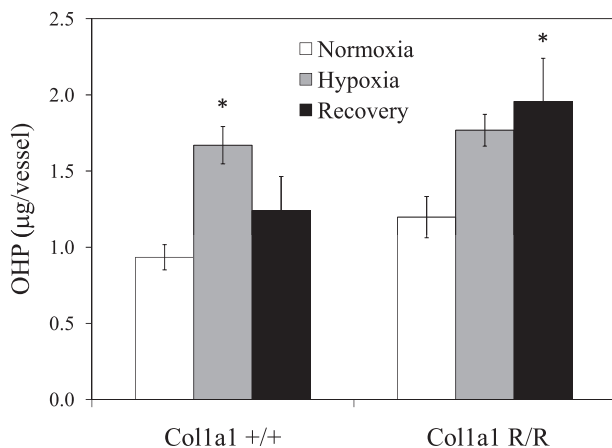

Fig. 7. PA hydroxyproline (OHP) content. Values are means ± SE; $N = 4$–7 per group. *$P < 0.05$ for hypoxia or recovery vs. normoxia.
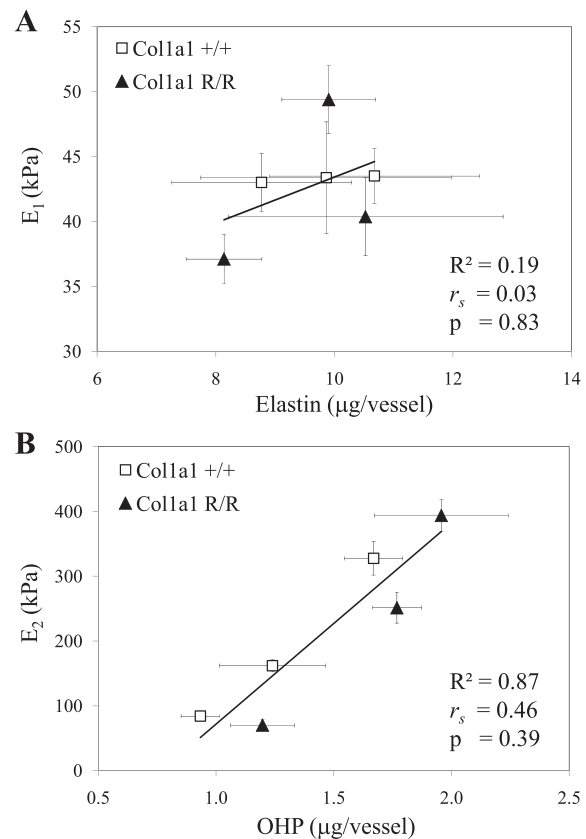
supports the important roles of both smooth muscle cell (SMC) apoptosis and collagen degradation in recovery (40).

Geometric changes of PAs. The remodeling of large-conduit PAs was confirmed by h measurements and histology. Both strains of mice showed increased h in response to hypoxia and reduced h after recovery (Figs. 2 and 3). These results are consistent with observations of hypoxia-induced remodeling in the conduit PAs of mice (20, 21), rats (4, 11), and calves (23).

Effects of hypoxia and recovery on arterial stiffness. In both Col1a1$^{+/+}$ and Col1a1$^{R/R}$ mice, chronic hypoxia decreased circumferential stretch (Fig. 4) and increased circumferential elastic modulus in a mid-to-high-strain range (E_2; Fig. 6B). It had no effect on circumferential elastic modulus in a low-strain range (E_1) in either mouse type (Fig. 6A). In previous studies on mice (20, 21), rats (4, 42), and calves (23), chronic hypoxia has been found to increase elastic modulus. In some of these studies, modulus in a low-strain range was calculated (20, 23), and in these cases chronic hypoxia increased the modulus. However, as we will discuss below, in both of these prior works, significant elastin changes were also found, which were correlated with the changes in low-strain modulus (20, 23).

With recovery, Col1a1$^{+/+}$ PA stretch and E_2 returned toward normal. In PA segments from rats, the elastance (slope of the pressure-volume relationship) (42) and wall stress (27) have previously been found to return to normal with recovery from hypoxia. As predicted, PA stretch and E_2 did not return to normal levels in Col1a1$^{R/R}$ mice. Indeed, PA stretch stayed at hypoxic levels, and E_2 increased further. Also, in the Col1a1$^{R/R}$ mice only, E_1 increased with recovery (Fig. 6A). We discuss

the likely biological explanations for these mechanical changes below.

Role of collagen content in arterial stiffness. In addition to decreasing arterial stretch and increasing mid-to-high-strain modulus, hypoxia induced collagen accumulation in Col1a1$^{+/+}$ mice and tended to increase collagen in the Col1a1$^{R/R}$ mice; increases in collagen with HPH were found previously in mice (20, 21) and rats (38). We hypothesized that, while breakdown of most extracellular matrix proteins (including collagen type I) would occur in Col1a1$^{+/+}$ PAs during recovery, the resistance of collagen type I to degradation in the Col1a1$^{R/R}$ mice would prevent the reduction in PA collagen content in this strain and cause persistent PA stiffening. We tested this hypothesis by correlating E_2 with collagen content (OHP). Previously, collagen content has been found to correlate well with mid-strain elastic modulus (21) and better with high-strain elastic modulus (20), whereas elastin content correlates well with changes in low-strain behavior (20, 23). We did not find a significant relationship between OHP and low-strain behavior (E_1) as expected, but did find a strongly linear but not significant relationship between collagen content and E_2 (Fig. 8). We attribute the lack of significance to several factors. First, as noted below, we were unable to perform a vessel-to-vessel correlation, which would have provided a more powerful test of the relationship. Second, the OHP assay ignores other potentially important changes in the extracellular matrix, such as cross-linking, changes in orientation, and changes in density (15). Nevertheless, the linear trend in the relationship supports our hypothesis.

The role of collagen in the increase in E_1 in the Col1a1$^{R/R}$ recovery group is unclear. One possibility is that increased activity of matrix-degrading enzymes in the Col1a1$^{R/R}$ mice altered the load-bearing capacity of elastin, such that the stiffer collagen fibers were recruited at lower loads.

Role of elastin content in arterial stiffness. The biochemical assay results for elastin suggest that the PA elastin content did not change with hypoxia or recovery for either strain of mice. On average, the elastin levels in single-mouse PAs were twice the detection limit of the Fastin elastin assay (5 μg), despite their small size and thin walls. In prior semiquantitative measurements of elastin by histology, our group showed that percent elastin in the extralobar PAs remained constant with hypoxia, but, because of wall thickening, elastin content increased (20, 21). Differences between the biochemical assay used here and previous histological measurements could be due to structural changes in elastic lamina that alter histological appearance without changing content. Prior studies using biochemical methods to determine the effect of chronic hypoxia on elastin content in extralobar arteries are not in agreement; using an assay for desmosine, Merklinger et al. (31) found no change, whereas Poiani et al. (38) found an increase.

All of these prior studies were performed in adult mice and rats. Studying the biomechanics of newborn calf extralobar arteries, Lammers et al. (23) showed a significant increase in low-strain elastic modulus with chronic hypoxia that was dependent on elastin. However, it is well known that newborn animals develop more severe pulmonary hypertension than adults with more dramatic vascular changes (36, 37, 45). Since the neonatal period is associated with significant elastin accumulation in the pulmonary trunk even in normoxic conditions

(24), elastin synthesis may be particularly sensitive to modulation by hypoxia during this time of rapid growth.

Role of cellular content in arterial stiffness. Direct quantification of PA SMC content was not performed in this study. While it has been demonstrated that hypoxia induces SMC hypertrophy and hyperplasia in intralobar PAs (17, 32), changes in SMC content or activity in extralobar PAs in response to hypoxia are not well studied. Previous work in our laboratory showed no significant changes in the SMC content of mouse extralobar PAs exposed to 10 days of hypoxia (20, 21). Here, we measured the vasoactive response of PAs isolated from Col1a1$^{+/+}$ and Col1a1$^{R/R}$ mice, but no changes were evident between groups or strains. These results suggest negligible changes in SMC content or activity in extralobar PAs in response to hypoxia and recovery.

Different remodeling responses to hypoxia in Col1a1$^{+/+}$ and Col1a1$^{R/R}$ mice. Because differences in PA pressure existed in normoxia between the two strains of mice, and because other potentially unknown consequences of the collagen type I defect could complicate the comparison, we focused our attention on comparisons between exposure conditions for each strain rather than between strains. However, we can make a few observations. First, the relative increase in E_2 with hypoxia is greater in the Col1a1$^{+/+}$ mice compared with the Col1a1$^{R/R}$ mice, but the greater relative increase in mean PA pressure in the Col1a1$^{R/R}$ strain would seem to suggest that the opposite should occur. One possible explanation is that, since the collagen degradation resistance of the Col1a1$^{R/R}$ mice impedes normal collagen turnover, it may prevent some degree of collagen synthesis during hypoxia, resulting in less vascular remodeling. This suggestion is consistent with the OHP results, where the average increase in collagen content in hypoxic Col1a1$^{R/R}$ PAs tended to be less than in hypoxic Col1a1$^{+/+}$ PAs, despite a larger increase in mean PA pressure.

Second, because of the greater increase in E_2 with hypoxia in the Col1a1$^{+/+}$ mice and smaller increase in E_2 with hypoxia, but continued increase in E_2 with recovery, in the Col1a1$^{R/R}$ mice, E_2 and the stress-strain curves are similar in the Col1a1$^{+/+}$ hypoxic and Col1a1$^{R/R}$ recovery groups. It is important to note, however, that the in vivo PA pressures in these two groups (Col1a1$^{+/+}$ hypoxic and Col1a1$^{R/R}$ recovery) are different (Table 1), so the in vivo behavior of these arteries should be quite different.

Third, we note that the trends in the relationships between E_2 and OHP suggest different slopes for the two mouse strains. In particular, for the same OHP value, E_2 tends to be higher in the Col1a1$^{+/+}$ arteries compared with the Col1a1$^{R/R}$ arteries. We speculate that the nongenetically modified form of collagen type I in the Col1a1$^{+/+}$ arteries is more effectively cross-linked than the defective collagen type I, but we did not quantify cross-link density in the present study.

Limitations and perspectives. In this study, we did not examine the changes in content of collagen subtypes (e.g., types I vs. III), but focused instead on the relationship between total collagen and PA stiffness. Since type I collagen is the major collagen subtype in PAs (3), a defect in type I collagen should translate into a defect in total collagen content. This has been largely confirmed by our results. Nevertheless, differences in collagen subtype content between the two strains in response to the defect may occur and may partly explain

baseline mechanobiological differences between PAs from Col1a1$^{R/R}$ and Col1a1$^{R/R}$ mice.

The results of collagen and elastin content assays were presented as microgram per vessel rather than per dry tissue weight. Vessels were dissected based on anatomic landmarks, and the same criteria for removing attached airway tissues were used. Despite this, OHP content was found to be dependent on the dissection technique of the individual experimenter, so we only present data for arteries harvested by one author (Z. Wang). Possibly due to the resulting smaller sample sizes and larger standard error, we were not able to obtain statistical significance for the increase in Col1a1$^{R/R}$ hypoxic group ($P = 0.14$). In addition, we were not able to do vessel- or mouse-specific mechanobiological correlations, as done previously (20, 21), which would have been more powerful. Nevertheless, the trends agreed with our expectations that changes in collagen content with hypoxia and recovery would follow changes in stiffness (mid-to-high-strain elastic modulus).

These results show that collagen content is important to PA stiffness. Potential adverse effects of PA stiffening are increased wave reflections and consequent right ventricular systolic dysfunction. If a similar relationship exists between collagen content and PA stiffness in patients with PA hypertension, anti-collagen accumulation agents (19, 37, 41, 43) might be an effective adjunct therapy worth pursuing.

DISCLOSURES

No conflicts of interest, financial or otherwise, are declared by the author(s).

REFERENCES

1. **Barbera JA, Peinado VI, Santos S.** Pulmonary hypertension in chronic obstructive pulmonary disease. *Eur Respir J* 21: 892–905, 2003.
2. **Beare AH, O'Kane S, Krane SM, Ferguson MW.** Severely impaired wound healing in the collagenase-resistant mouse. *J Invest Dermatol* 120: 153–163, 2003.
3. **Diez J.** Arterial stiffness and extracellular matrix. *Adv Cardiol* 44: 76–95, 2007.
4. **Drexler ES, Bischoff JE, Slifka AJ, McCowan CN, Quinn TP, Shandas R, Ivy DD, Stenmark KR.** Stiffening of the extrapulmonary arteries from rats in chronic hypoxic pulmonary hypertension. *Journal of Research of the National Institute of Standards and Technology* 113: 239–249, 2008.
5. **Edwards CA, O'Brien WD Jr.** Modified assay for determination of hydroxyproline in a tissue hydrolyzate. *Clin Chim Acta* 104: 161–167, 1980.
6. **Estrada KD, Chesler NC.** Collagen-related gene and protein expression changes in the lung in response to chronic hypoxia. *Biomech Model Mechanobiol* 8: 263–272, 2009.
7. **Fagan KA, Fouty BW, Tyler RC, Morris KG Jr, Hepler LK, Sato K, LeCras TD, Abman SH, Weinberger HD, Huang PL, McMurtry IF, Rodman DM.** The pulmonary circulation of homozygous or heterozygous eNOS-null mice is hyperresponsive to mild hypoxia. *J Clin Invest* 103: 291–299, 1999.
8. **Faury G, Maher GM, Li DY, Keating MT, Mecham RP, Boyle WA.** Relation between outer and luminal diameter in cannulated arteries. *Am J Physiol Heart Circ Physiol* 277: H1745–H1753, 1999.
9. **Fonck E, Prod'hom G, Roy S, Augsburger L, Rufenacht DA, Stergiopulos N.** Effect of elastin degradation on carotid wall mechanics as assessed by a constituent-based biomechanical model. *Am J Physiol Heart Circ Physiol* 292: H2754–H2763, 2007.
10. **Fraser KL, Tullis DE, Sasson Z, Hyland RH, Thornley KS, Hanly PJ.** Pulmonary hypertension and cardiac function in adult cystic fibrosis: role of hypoxemia. *Chest* 115: 1321–1328, 1999.
11. **Fung YC, Liu SQ.** Changes of zero-stress state of rat pulmonary arteries in hypoxic hypertension. *J Appl Physiol* 70: 2455–2470, 1991.
12. **Gan CT, Lankhaar JW, Westerhof N, Marcus JT, Becker A, Twisk JW, Boonstra A, Postmus PE, Vonk-Noordegraaf A.** Noninvasively assessed pulmonary artery stiffness predicts mortality in pulmonary arterial hypertension. *Chest* 132: 1906–1912, 2007.
13. **Hiestand D, Phillips B.** The overlap syndrome: chronic obstructive pulmonary disease and obstructive sleep apnea. *Crit Care Clin* 24: 551–563, vii, 2008.
14. **Humphrey JD.** *Cardiovascular Solid Mechanics: Cells, Tissues and Organs*. New York: Springer-Verlag, 2002.
15. **Humphrey JD.** Mechanisms of arterial remodeling in hypertension: coupled roles of wall shear and intramural stress. *Hypertension* 52: 195–200, 2008.
16. **Incalzi RA, Fuso L, De Rosa M, Di Napoli A, Basso S, Pagliari G, Pistelli R.** Electrocardiographic signs of chronic cor pulmonale: a negative prognostic finding in chronic obstructive pulmonary disease. *Circulation* 99: 1600–1605, 1999.
17. **Jeffery TK, Morrell NW.** Molecular and cellular basis of pulmonary vascular remodeling in pulmonary hypertension. *Prog Cardiovasc Dis* 45: 173–202, 2002.
18. **Kass DA.** Age-related changes in venticular-arterial coupling: pathophysiologic implications. *Heart Fail Rev* 7: 51–62, 2002.
19. **Kerr JS, Riley DJ, Frank MM, Trelstad RL, Frankel HM.** Reduction of chronic hypoxic pulmonary hypertension in the rat by beta-aminopropionitrile. *J Appl Physiol* 57: 1760–1766, 1984.
20. **Kobs RW, Chesler NC.** The mechanobiology of pulmonary vascular remodeling in the congenital absence of eNOS. *Biomech Model Mechanobiol* 5: 217–225, 2006.
21. **Kobs RW, Muvarak NE, Eickhoff JC, Chesler NC.** Linked mechanical and biological aspects of remodeling in mouse pulmonary arteries with hypoxia-induced hypertension. *Am J Physiol Heart Circ Physiol* 288: H1209–H1217, 2005.
22. **Lakes RS.** *Viscoelastic Solids*. Boca Raton, FL: CRC, 1998.
23. **Lammers SR, Kao PH, Qi HJ, Hunter K, Lanning C, Albietz J, Hofmeister S, Mecham R, Stenmark KR, Shandas R.** Changes in the structure-function relationship of elastin and its impact on the proximal pulmonary arterial mechanics of hypertensive calves. *Am J Physiol Heart Circ Physiol* 295: H1451–H1459, 2008.
24. **Leung DY, Glagov S, Mathews MB.** Elastin and collagen accumulation in rabbit ascending aorta and pulmonary trunk during postnatal growth. Correlation of cellular synthetic response with medial tension. *Circ Res* 41: 316–323, 1977.
25. **Li X, Zhang X, Leathers R, Makino A, Huang C, Parsa P, Macias J, Yuan JX, Jamieson SW, Thistlethwaite PA.** Notch3 signaling promotes the development of pulmonary arterial hypertension. *Nat Med* 15: 1289–1297, 2009.
26. **Li Z, Huang W, Jiang ZL, Gregersen H, Fung YC.** Tissue remodeling of rat pulmonary arteries in recovery from hypoxic hypertension. *Proc Natl Acad Sci U S A* 101: 11488–11493, 2004.
27. **Liu SQ.** Regression of hypoxic hypertension-induced changes in the elastic laminae of rat pulmonary arteries. *J Appl Physiol* 82: 1677–1684, 1997.
28. **Liu X, Wu H, Byrne M, Jeffrey J, Krane S, Jaenisch R.** A targeted mutation at the known collagenase cleavage site in mouse type-I collagen impairs tissue remodeling. *J Cell Biol* 130: 227–237, 1995.
29. **London GM, Marchais SJ, Guerin AP, Pannier B.** Arterial stiffness: pathophysiology and clinical impact. *Clin Exp Hypertens* 26: 689–699, 2004.
30. **Mahapatra S, Nishimura RA, Sorajja P, Cha S, McGoon MD.** Relationship of pulmonary arterial capacitance and mortality in idiopathic pulmonary arterial hypertension. *J Am Coll Cardiol* 47: 799–803, 2006.
31. **Merklinger SL, Wagner RA, Spiekerkoetter E, Hinek A, Knutsen RH, Kabir MG, Desai K, Hacker S, Wang L, Cann GM, Ambartsumian NS, Lukanidin E, Bernstein D, Husain M, Mecham RP, Starcher B, Yanagisawa H, Rabinovitch M.** Increased fibulin-5 and elastin in

S100A4/Mts1 mice with pulmonary hypertension. *Circ Res* 97: 596–604, 2005.

32. **Meyrick B, Reid L.** Hypoxia-induced structural changes in the media and adventitia of the rat hilar pulmonary artery and their regression. *Am J Pathol* 100: 151–178, 1980.

33. **Mitchell GF, Tardif JC, Arnold JM, Marchiori G, O'Brien TX, Dunlap ME, Pfeffer MA.** Pulsatile hemodynamics in congestive heart failure. *Hypertension* 38: 1433–1439, 2001.

34. **Molthen RC, Karau KL, Dawson CA.** Quantitative models of the rat pulmonary arterial tree morphometry applied to hypoxia-induced arterial remodeling. *J Appl Physiol* 97: 2372–2384; discussion 2354, 2004.

35. **Murphy G, Docherty AJ.** The matrix metalloproteinases and their inhibitors. *Am J Respir Cell Mol Biol* 7: 120–125, 1992.

36. **Peterson LH, Jensen RE, Parnell J.** Mechanical properties of arteries in vivo. *Circ Res* 8: 622–639, 1960.

37. **Poiani GJ, Tozzi CA, Choe JK, Yohn SE, Riley DJ.** An antifibrotic agent reduces blood pressure in established pulmonary hypertension in the rat. *J Appl Physiol* 68: 1542–1547, 1990.

38. **Poiani GJ, Tozzi CA, Yohn SE, Pierce RA, Belsky SA, Berg RA, Yu SY, Deak SB, Riley DJ.** Collagen and elastin metabolism in hypertensive pulmonary arteries of rats. *Circ Res* 66: 968–978, 1990.

39. **Prockop DJ, Kivirikko KI.** Collagens: molecular biology, diseases, and potentials for therapy. *Annu Rev Biochem* 64: 403–434, 1995.

40. **Riley DJ, Thakker-Varia S, Wilson FJ, Poiani GJ, Tozzi CA.** Role of proteolysis and apoptosis in regression of pulmonary vascular remodeling. *Physiol Res* 49: 577–585, 2000.

41. **Simon PM, Pachence J, Belinka B, Poiani GJ, Lu SE, Tozzi CA, Riley DJ.** Prodrug of proline analogue reduces hypoxic pulmonary hypertension in rats. *Pulm Pharmacol Ther* 19: 242–250, 2006.

42. **Tozzi CA, Christiansen DL, Poiani GJ, Riley DJ.** Excess collagen in hypertensive pulmonary arteries decreases vascular distensibility. *Am J Respir Crit Care Med* 149: 1317–1326, 1994.

43. **Tozzi CA, Poiani GJ, McHugh NA, Shakarjian MP, Grove BH, Samuel CS, Unemori EN, Riley DJ.** Recombinant human relaxin reduces hypoxic pulmonary hypertension in the rat. *Pulm Pharmacol Ther* 18: 346–353, 2005.

44. **Tuchscherer HA, Vanderpool RR, Chesler NC.** Pulmonary vascular remodeling in isolated mouse lungs: effects on pulsatile pressure-flow relationships. *J Biomech* 40: 993–1001, 2007.

45. **Tucker A, Migally N, Wright ML, Greenlees KJ.** Pulmonary vascular changes in young and aging rats exposed to 5,486 m altitude. *Respiration* 46: 246–257, 1984.

46. **Vuorio E, de Crombrugghe B.** The family of collagen genes. *Annu Rev Biochem* 59: 837–872, 1990.

47. **Woessner JF Jr.** The determination of hydroxyproline in tissue and protein samples containing small proportions of this amino acid. *Arch Biochem Biophys* 93: 440–447, 1961.

48. **Zhao J, Day J, Yuan ZF, Gregersen H.** Regional arterial stress-strain distributions referenced to the zero-stress state in the rat. *Am J Physiol Heart Circ Physiol* 282: H622–H629, 2002.

49. **Zhao W, Byrne MH, Boyce BF, Krane SM.** Bone resorption induced by parathyroid hormone is strikingly diminished in collagenase-resistant mutant mice. *J Clin Invest* 103: 517–524, 1999.